

02-027

HOW DO URBAN FORM AND SOCIOECONOMIC DIFFERENCES AFFECT THE TEMPERATURE OF THE RESIDENTIAL DISTRICT?

López-Guerrero, Rafael E. ⁽¹⁾; Verichev, Konstantin ⁽²⁾; Castro, Alexandre ⁽³⁾; Carpio, Manuel ⁽⁴⁾

(1) Pontificia Universidad Católica de Chile, ⁽²⁾ Universidad Austral de Chile, ⁽³⁾

Universidade Federal do Rio Grande do Norte, ⁽⁴⁾ Pontificia Universidad Católica de Chile & Centro Nacional de Excelencia para la Industria de la Madera (CENAMAD)

Urban temperature is crucial to reach world sustainable development goals. This could affect building energy consumption and human thermal comfort, among other social, economic, and environmental issues. Meanwhile, cities can aggravate such problems by generating the phenomenon of urban heat islands (UHI). The main purpose of this research is to classify the urban form of Temuco city, Chile, and simulate the urban temperatures in several socioeconomic districts to understand how these differences could affect the neighborhoods in terms of house-building energy and thermal performance. For this, the local climate zone classification methodology was applied, then the urban weather generator (UWG) software was used to perform the different climate files. Also, data loggers were installed in the studied districts to validate the simulations in UWG. The results showed that low-income neighborhoods have higher UHI intensity reaching 9.5°C, while high-income neighbourhoods have UHI intensity as high as 5°C. These results can strongly affect the building energy performance in energy-vulnerable districts once all cities have the same energy and thermal official standards. Future investigations will be carried out to better understand how housing stock is affected.

Keywords: sustainability; urban form; socioeconomic differences; energy performance; urban heat island.

¿CÓMO AFECTAN LA FORMA URBANA Y LAS DIFERENCIAS SOCIOECONÓMICAS A LA TEMPERATURA DE UN DISTRITO RESIDENCIAL?

La temperatura urbana es crucial para alcanzar los objetivos mundiales de desarrollo sostenible. Esto podría afectar el consumo de energía de los edificios y el confort térmico humano, entre otros problemas sociales, económicos y ambientales. Mientras tanto, las ciudades pueden agravar tales problemas al generar el fenómeno de las islas de calor urbanas (UHI). El objetivo principal de esta investigación es clasificar la forma urbana de la ciudad de Temuco, Chile, y simular las temperaturas urbanas en varios distritos socioeconómicos para comprender cómo estas diferencias podrían afectar los barrios en términos de rendimiento energético y térmico de la construcción de viviendas. Se aplicó la metodología de clasificación de zonas climáticas locales, luego se utilizó el software generador de clima urbano (UWG) para los diferentes archivos climáticos. Además, se instalaron registradores de datos para validar las simulaciones en UWG. Los resultados mostraron que los barrios de bajos ingresos tienen una mayor intensidad de UHI que alcanza los 9.5 °C, mientras que los barrios de altos ingresos tienen una intensidad de UHI de hasta 5 °C. Estos resultados pueden afectar el rendimiento energético de los edificios en distritos energéticamente vulnerables siempre que todas las ciudades tengan los mismos estándares oficiales.

Palabras clave: sostenibilidad; forma urbana; diferencias socioeconómicas; rendimiento energético; isla de calor urbana

Agradecimientos: This work was funded by the National Agency for Research and Development (ANID) of Chile through the projects ANID BASAL FB210015 CENAMAD and ANID FONDECYT 1201052.



© 2023 by the authors. Licensee AEIPRO, Spain. This article is licensed under a Creative Commons Attribution-NonCommercial-NoDerivatives 4.0 International License (<https://creativecommons.org/licenses/by-nc-nd/4.0/>).

1. Introduction

Cities are crucial in achieving the global goals of reducing global warming and sustainable development (Bazaz et al., 2018; UN, 2015), because although they occupy only 3% of the Earth's surface, they account, on average, for 70% of energy consumption and 75% of carbon emissions in the world (C40 Cities, 2016; IEA, 2020; ONE-Habitat, 2019). Further, 55% of the human population lives in cities, and it is expected that by 2050, this proportion will increase to 68% (UN, 2018). This expected population increase varies in different regions of the world. For example, in Latin America and the Caribbean, the current urban population is 80.7% (the year 2018) and will be 87.8% by 2050 (UN, 2018), and urban growth is expected to be greater (up to 95%) in small- and medium-sized cities in developing countries (UN, 2018; Roy, J. et al., 2018). Thus, the effects produced by this growth phenomenon could increase the vulnerability of cities and affect a greater number of people. Cities could also contribute to increasing the phenomenon of local and global climate change to a greater extent (Khan et al., 2021).

Further, cities characteristically produce the urban heat island (UHI) effect, which is understood as rising temperatures in urban areas in relation to surrounding rural areas (Oke et al., 2017). UHI intensity (UHII) is defined as the differential of both temperatures (urban and adjacent rural) (Zhou et al., 2015). The causes of UHI are associated with various causes, including land use change (replacement of natural covers by non-permeable surfaces), properties of building materials (e.g. low albedo and high thermal inertia), change in roughness and morphology (which inhibits, for example, natural ventilation), and anthropogenic heat generation (heat emitted by buildings, people, transport, and industries) (Hong et al., 2020; Woong Kim & Brown, 2021). UHI is associated with various socio-environmental and economic impacts, including an increase in photochemical smog and urban pollution (Li et al., 2018; Ulpiani, 2021), among other effects. Buildings in urban environments are affected by UHIs, the impacts of which vary from -20% to 345%, with an average 23.2% increase in cooling energy consumption and an average 18% decrease in heating energy consumption (López-Guerrero et al., 2022). Therefore, the study of UHI and its effects is fundamental for proposing better urban living conditions and diminishing sustainability impacts.

1.2 Objectives

With the intention of analysing how UHI could affect the thermo-energy performance of buildings in a southern Latin American city, this research presents the initial results of the analysis carried out regarding the urban form and the UHII in the most representative urban tissues in the study case. For this, Temuco City (Chile) was selected, considering the scarcity of studies in UHI with Csb climates according to Köppen-Geiger (López-Guerrero et al., 2022; Ulpiani, 2021) and the high UHII of the city (Martinez-soto et al., 2021). Further, the city is not located on the Chilean coast, an area that has already been studied in similar research (Palme et al., 2017). The city was classified into local climate zones (LCZ) (Stewart & Oke, 2012), and the UHII was modelled with urban weather generation (UWG) software (Bueno et al., 2013). The results were compared with the socioeconomic levels of two residential districts to identify and discuss potential differences that may affect the housing stock.

2. Methodology

2.1 Study Area

The city of Temuco is the capital of Araucanía Region located in southern Chile (longitude 38.76°E; latitude 72.63°S). According to official population projections, Temuco is a mid-sized city with 308,175 inhabitants (INE, 2017). The city is characterised by warm and temperate summers and rainy winters. The average annual temperature is 11.4°C, and there is approximately 1482 mm of precipitation. It is further classified as Csb according to the Köppen-Geiger climate classification (Climate data, 2023; Peel et al., 2007).

2.2 LCZ Mapping

LCZ is a standard and international classification system for urban tissues (Stewart & Oke, 2012). The method allows for dividing a city into homogeneous parameters related to morphology, building density, urban land uses, and other urban and building properties. This scheme allows evaluation of the impact of urban microclimates on building thermos-energy performance (Yang et al., 2020). In this study, LCZ mapping was performed in two ways: manual mapping and using an improved method of the world urban database and portal tool (WUDAPT) with Landsat satellite images (Bechtel et al., 2015, 2019). For manual mapping, several campaigns and data collection were carried out.

LCZ classification requires 10 urban parameters that determine every LCZ class: (i) sky view factor, (ii) canyon aspect ratio, (iii) mean building height, (iv) terrain roughness class, (v) building surface fraction, (vi) impervious surface fraction, (vii) pervious surface fraction, (viii) surface admittance, (ix) surface albedo, and (x) anthropogenic heat flux. The sky view factor was estimated by means of fisheye lens photography of representative streets in every urban area, and then processing the images with RayMan Software algorithm (Matzarakis et al., 2006). The Canyon aspect ratio was similarly calculated by sampling typical streets during the field campaigns. The mean building height was extracted from the local urban database (Municipalidad de Temuco, 2015) and compared with Google Street View. Terrain roughness class was defined according to the Davenport classification (Davenport G. et al., 2000). Building surface fraction, impervious surface fraction, and pervious surface fraction were obtained by analysis of normalised difference built-up index (NDBI), normalised difference vegetation index (NDVI) from Landsat 8 and Sentinel high resolution satellite images, and CAD mapping from local database (Municipalidad de Temuco, 2015). Anthropogenic heat flux from vehicular sources was calculated using a previously proposed method (Grimmond, 1992; Quah & Roth, 2012). However, in this study, surface admittance, albedo, and anthropogenic heat flux from sources other than vehicular traffic were not calculated because of a lack of data from the studied area.

2.3 UHI Modelling

For the estimation of urban weather data, this study used the Urban Weather Generator V 4.1 (UWG) tool. This software couples an atmospheric model with a building simulation model, using a parametric reading of the urban area, and a rural weather file, to generate new urban weather files that consider the UHI effect for the climatic variable's outputs (Bueno et al., 2013). This software has been widely used and validated in previous studies (Bueno et al., 2014; Mao et al., 2017; Salvati et al., 2019). The inputs required in UWG are divided into several categories: microclimate parameters, urban characteristics, vegetation parameters, and building surfaces and typologies. However, the most sensitive input parameters have been previously identified

(Nakano et al., 2015; Salvati et al., 2019) and are typically calculated for the most representative urban areas. According to these studies, the main parameters are average building height, site coverage ratio, façade-to-site ratio. These parameters were manually estimated using the same methods mentioned in LCZ mapping, based on official local data and high-resolution satellite images (Municipalidad de Temuco, 2015). Similarly, urban area vegetation coverage, urban area vegetation trees, and sensible anthropogenic heat were estimated. Anthropogenic heat from vehicular traffic was calculated using a previously proposed method (Grimmond, 1992; Quah & Roth, 2012). Building surfaces were calculated using high-resolution satellite images and Computer-Aided Drafting (CAD) urban maps provided by previous local research (Municipalidad de Temuco, 2015). Building properties were customised according to Chilean local standards (Ordenanza General de Urbanismo y Construcciones, 2022) for the thermal zone corresponding to Temuco City (zone 5-F). It is important to highlight that Temuco city cooling uses are very low (Corporación de Desarrollo Tecnológico, 2019); thus, cooling setpoints were scheduled as 35°C for the whole day.

2.4 Field Measurements

Considering the local UHI estimations, it is important to obtain data from field measurements for comparison of every urban area mapped in the LCZ scheme and modelled in UWG. For this, several sensors of relative humidity (RH) and temperature (°C) were installed in the studied area. Thus, a six-sensor model HOBO MX 2302A with accuracy of +/- 0.2°C and +/- 2.5% RH was installed in the most representative LCZ. According to Stewart and Oke (2012), the typical circle of influence of every sensor has a radius of 200–500 m (Stewart & Oke, 2012). Thus, considering the scale of every LCZ in Temuco, one sensor was installed for each zone. The sensors were installed 2 m above ground, far from any artificial heat source and at least 2.5 m from any obstacle (roofs and walls), normally in front garden spaces, and were protected by solar radiation shields (Oke, 2006). Similarly, another datalogger was installed in a rural area in the southeast, 8 km (straight line) from the centre of Temuco. Moreover, weather data was obtained from the Maquehue meteorological station, which is in the southwest, 5 km from the centre of Temuco (straight line) (Fig. 1). This is the nearest rural meteorological station to Temuco (Meteochile, 2023). Both field measurements were used as rural temperature references. Finally, to better understand the relationship between LCZ and socioeconomic levels in Temuco City, the MMQGIS plugin, available in QGIS software, was used to perform spatial data fusion of LCZ and socioeconomic classes. Thus, comparisons were made between the data on the scale of urban blocks to identify congruences and inconsistencies.

3. Results

Temuco City was mapped according to LCZ classification. Fig. 1a shows the LCZ map obtained via satellite images and WUDAPT algorithms. This was executed according to the methodology proposed by portal WUDADT. After several iterations, an overall accuracy of 0.70 was achieved. As shown in the figure, using this method, the main LCZ classes detected by the algorithms are LCZ6 and LCZ3, with smaller parts of LCZ2 and LCZ5. Therefore, to obtain the actual urban characteristics of Temuco, a manual LCZ map was performed according to the proposed methodology. This decision was made because of the heterogeneous urban characteristics of Temuco. Thus, the LCZ subclass was shaped, which allowed combining the characteristics of two different classes for better representation of actual urban conditions (Stewart & Oke, 2012). Fig. 1b shows the manually configured LCZ map. Here, four types are predominant: LCZ23, LCZ6, LCZ6₃, and LCZ6₅. These classes were used for further analysis. Table 1 shows the main

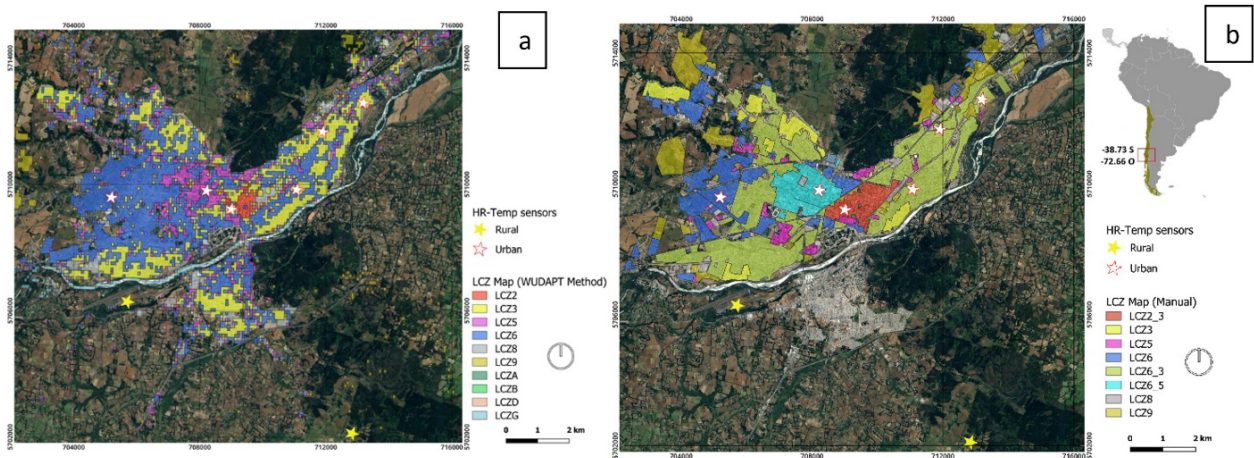
LCZ classes in Temuco and its calculated properties in an area of 0.25 km² (500 × 500 m) of each urban tissue. Table 2 shows the socioeconomic levels associated with each LCZ. These levels were officially defined in the last census of the country and include five categories of high- to low-income levels, designated as ABC1, C2, C3, D, and E (INE, 2017).

Table 1: Manually Mapped Main Local Climate Zones (LCZ) in Temuco.

LCZ class	Satellite image	Low-level photograph	Properties*
LCZ2 3		 <small>PUC Zonas Climáticas Locales De Temuco 40 10.5021 14.16 -38 74016 -72.59227 (17m) Altitud: 131m</small>	SVF = 0.46 H/W = 0.7–1.2 MBH = 14 TRC = 6–7 BSF = 42% ISF = 47% AHF = 35.51 SCR = 0.83 FSR = 1.01 SEL = C2–C3 LCU = Commercial/Residential
LCZ6			SVF = 0.68 H/W = 0.3 MBH = 3.5 TRC = 5 BSF = 27% ISF = 22% AHF = 0.96 SCR = 0.51 FSR = 0.57 SEL = ABC1–C2 LCU = Residential
LCZ6 3			SVF = 0.62 H/W = 0.3–0.55 MBH = 3.5 TRC = 6 BSF = 35% ISF = 38% AHF = 14.18 SCR = 0.82 FSR = 0.68 SEL = D–E LCU = Residential
LCZ6 5			SVF = 0.54 H/W = 0.3–0.8 MBH = 10 TRC = 5–6 BSF = 28% ISF = 33% AHF = 28.07 SCR = 0.37 FSR = 0.82 SEL = ABC1–C2 LCU = Commercial/Residential

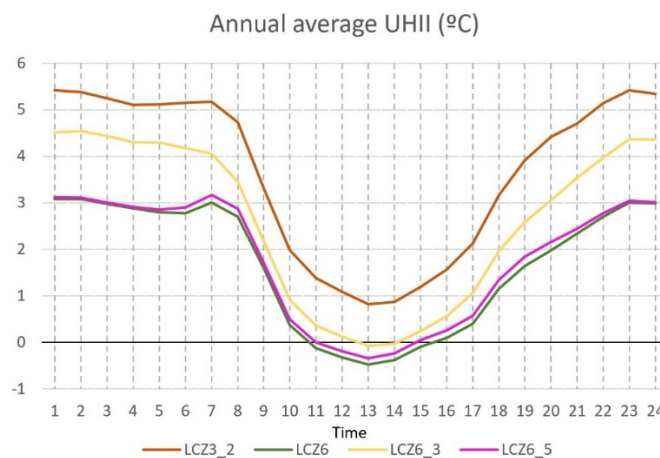
Notes: SVF = sky view factor, H/W = canyon aspect ratio, MBH = mean building height, TRC = terrain roughness class, BSF = building surface fraction, ISF = impervious surface fraction, AHF = anthropogenic heat flux, SCR = site coverage ratio, FSR = façade-to-site ratio, SEL = socioeconomic level, LCU = land cover use. (*) Most of the values are averages of 0.25 km² of each urban area, except for AHF, which is vehicular traffic peak emissions. Image references: Google Images.

Figure 1: Main Local Climate Zones (LCZ) Mapped Using WUDAPT Methodology (A) and Manually (b)



Some of the values shown in Table 2 (MBH, SCR, FSR, and AFH) were used as input in UWG to calculate the UHI for each LCZ. The annual average of the UHI is shown in Figure 2. As expected, higher temperatures were exhibited by LCZ3₂ and LCZ6₃. Due to the lack of urban greenery, the higher site coverage, and façade-to-site ratios here, the UHI might reach 5.4°C and 4.5°C more than the urban areas, respectively. LCZ6 and LCZ6₅ are quite similar, highlighting the sensitivity of UHI to SCR values, as demonstrated in previous research (Nakano et al., 2015; Salvati et al., 2019). It is interesting to note that the LCZ classes with more urban vegetation might show urban cold islands in the hours near noon.

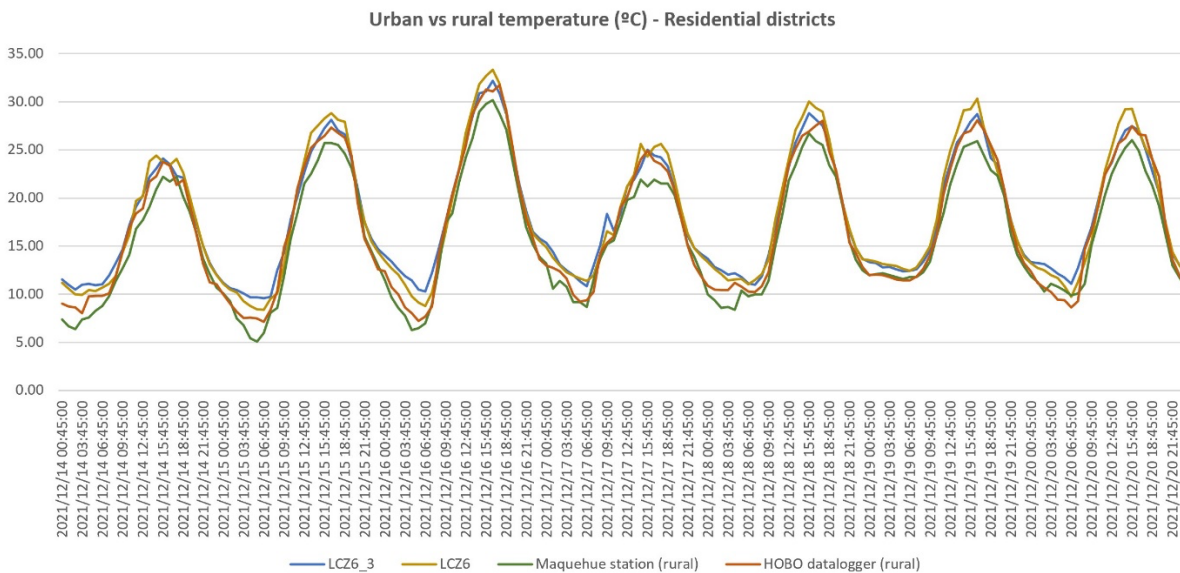
Figure 2: Annual Average of UHI in the Main Local Climate Zones (LCZ) of Temuco



To compare the modelled UHI with the empirical data, measurements were carried out in every LCZ. Similarly, two rural measurements were used for comparison (Fig. 1). Thus, data from the Maquehue station and data collected from the rural datalogger were compared using root mean square error (RMSE) and mean absolute percentage error (MAPE). Temperatures in the rural HOBO datalogger were taken from December 2021 to June 2022 (six months), and these data were compared with the same timeframe extracted from the Maquehue station. The results show an RMSE of 1.6 and a MAPE of 7.8%, which values are in an acceptable range compared with similar literature (Bueno et al., 2013; Litardo et al., 2020). This error is caused by differences in instruments and locations.

As shown in Tables 1 and 2, LCZ6 and LCZ6₃ contain mainly residential areas but with different socioeconomic levels. LCZ6 principally encompasses medium- and high-income levels, and LCZ6₃ covers low-income levels. To compare these two different residential areas, Fig. 3 shows the measured urban temperature and rural references during the first whole week recorded in this study (December 14 to December 21, 2021). Here, some differences in trend are observed in comparison with the UHI modelled in Figure 2, in which LCZ6₃ showed higher temperatures, followed by LCZ6 and rural references. According to Fig. 3, LCZ6 temperatures were slightly higher than those of LCZ6₃ in the day hours, with an opposite trend in the night-time on most day of the days shown. The UHI average was calculated for the entire season of summer metred (from 14 December 2021 to 31 March 2022). LCZ6 exhibited an average UHI of 1.58°C (compared with rural Maquehue station) and 0.92°C (compared with rural HOBO measurements). By contrast, LCZ6₃ had an average UHI of 1.62°C and 0.96°C, respectively. This similar average can be explained by the trend shown in Fig. 3, which was maintained during the season, in which daytime temperatures were offset by night-time temperatures.

Figure 3: Urban and Rural Temperatures in Two Different Residential Districts (LCZ6 and LCZ6₃)



Finally, Table 2 shows the number of blocks per LCZ and socioeconomic level (SEL). According to the data, the higher-income classes (A, B, and C1) are mostly located in the LCZ6 class, where there is a lower building density, greater dispersion of the urban fabric, and streets in a configurational grid pattern. By contrast, LCZ3 and LCZ6₃ tend to represent the low-income districts in the studied city, where urban vegetation is lesser and the site coverage ratio is higher.

Table 2: Number of Urban Blocks Per Local Climatic Zone (LCZ) and Socioeconomic Level.

SEL	Number of Blocks per Zone							
	LCZ2 ₃	LCZ3	LCZ5	LCZ6	LCZ6 ₃	LCZ6 ₅	LCZ8	LCZ9
ABC1	2	1	0	123	72	18	0	59
C2	57	21	5	144	366	57	0	25
C3	44	155	7	171	651	19	3	29
D	7	139	2	103	559	1	3	33
E	1	128	0	8	234	0	0	1

4. Discussion

This study analysed the urban tissue characteristics of Temuco city in Chile to understand how the urban microclimate is influenced by different local climate zones and affects the thermal balance of two districts of different socioeconomic levels. Two different LCZ mapping methods were used. The findings suggest that for the city studied, the best way to analyze real urban morphology is using an LCZ map mapped manually, as the WUDAPT method does not allow for the creation of heterogeneous LCZ classes. Although time-consuming, the LCZ map manually configured better describes the complex urban tissue, especially in Latin American cities where, historically, growth and expansion used are typically irregular or even disordered (UN-HABITAT, 2012).

UHI simulations were also modelled in the main LCZ classes in Temuco. As expected, the results showed a higher urban temperature in denser urban areas (LCZ2₃). However, in the comparison of similar LCZ classes, important differences were found in the modelled UHI. LCZ6 and LCZ6₃ contain the same land use; however, the former exhibited a lower average UHI. This outcome is due to the presence of more urban vegetation and less building density in LCZ6 compared to LCZ6₃. In this study, the comparison of metred temperatures with modelled temperatures also revealed some differences caused by the timeframe and representation of the UWG outputs. UWG uses a new EnergyPlus weather (EPW) file, which is based in a typical weather year and thus represents several years, unlike the metred temperatures in this study. However, metred temperatures in LCZ6 and LCZ6₃ exhibited results similar to modelled temperatures (Fig. 2), as LCZ6₃ had higher nighttime temperatures compared with LCZ6, confirming that parts of the city have elevated UHI in night hours.

By contrast, Table 2 shows that lower SEL (C2, C3, D, and E) are more predominant in the LCZ6₃ class, characterised by their moderate density, mixed land use, and a combination of built and natural features. From a microclimate perspective, LCZ6₃ areas in Temuco tend to be characterised by a low amount of vegetation cover, low levels of impervious surface cover, and relatively high levels of surface roughness. These factors, along with the moderate building heights, can create a moderate UHI. Similarly, the LCZ3 class is more predominant in lower-income classes. LCZ3 areas tend to be characterised by a high amount of impervious surface cover, with limited vegetation cover. The tall buildings and narrow streets can also create a significant UHI (Fig. 2). This means that areas with characteristics that tend to have less environmental comfort are favoured in poorer regions.

LCZ6₅ classes are more predominant in higher-income neighbours. In the LCZ6₅ class, the dominant land use is residential, with buildings typically no higher than two to three floors. The

buildings are usually single-family homes or medium- and low-rise apartment buildings surrounded by spacious yards, parks, and green spaces. The streets in LCZ6₅ areas are typically wider and more regular than those in other LCZ types, with a mix of local and arterial roads. LCZ6₅ areas tend to be characterised by a high amount of vegetation cover, low levels of impervious surface cover, and relatively low levels of surface roughness. These factors, along with the low building heights, can create a cooler and more comfortable microclimate compared to other urban areas.

These outcomes demonstrate that urban areas with higher incomes have a milder microclimate that provides a greater sense of comfort than areas with lower incomes in Temuco. The richest social classes in the city settle near amenities and with urbanisation standards that provide greater environmental comfort. Thus, special attention should be paid to low-income districts, as they could suffer high UHI, whereas the housing stock is poorer in terms of materiality and the thermal conditions of envelopes. Moreover, low-income neighbourhoods typically suffer from energy poverty, which is another socioeconomic issue in the southern cities of Chile (Pérez-Fargallo et al., 2020). Even though UHI alleviates heating energy consumption expenses, cooling loads might rise, which will produce the necessity of cooling energy consumption or poorer thermal comfort conditions, especially for populations with more financial constraints. Moreover, the UHI analysed in this study was shown to be higher during night hours when occupancy in residential districts increased, thus aggravating the aforementioned issues. Finally, it is important to highlight that UHI consequences might worsen considering future scenarios of global warming, as was demonstrated in previous research in the studied city (Verichev & Carpio, 2020).

5. Conclusions

Cities and the understanding of urban thermal behaviour are complex tasks. Urban microclimates depend on several factors acting simultaneously. Here, LCZ was demonstrated to be an efficient methodology for analysing these issues. This research evaluated the relationship between the LCZ, UHI phenomena, and socioeconomic levels of residential neighbourhoods in Temuco city of Chile. When LCZ maps and SEL classification overlapped, the results showed a correlation between the LCZ classes with lesser urban vegetation, higher building density, and the presence of a low socioeconomic class in some districts. In this sense, the findings show that low-income neighbourhoods exhibited higher nocturnal UHI. The consequences of these results are more challenging in residential districts because the concentrated schedule uses night time hours. Moreover, low-income districts are usually made up of deficient building envelopes and other energy poverty difficulties. These results should be considered in public policies and energy standards planning, as UHI is typically not part of local energy performance regulations or state policies for land-use analysis of different urban tissues. Future research could be carried out using indoor thermal and energy analysis or energy modelling of different house configurations to better elucidate how UHI affects living conditions at different socioeconomic levels.

References

Bazaz, A., Bertoldi, P., Buckeridge, M., Cartwright, A., Coninck, H. de, Engelbrecht, F., Jacob, D., Hourcade, J.-C., Klaus, I., Kleijne, K. de, Lwasa, S., Markgraf, C., Newman, P., Revi, A., Rogelj, J., Schultz, S., Shindell, D., Singh, C., Solecki, W., ... Waisman, H. (2018).

Summary for Urban Policymakers: What the IPCC Special Report on 1.5 C means for Cities (Issue December 2018). <https://doi.org/10.24943/SCPM.2018>

- Bechtel, B., Alexander, P. J., Beck, C., Böhner, J., Brousse, O., Ching, J., Demuzere, M., Fonte, C., Gál, T., Hidalgo, J., Hoffmann, P., Middel, A., Mills, G., Ren, C., See, L., Sismanidis, P., Verdonck, M. L., Xu, G., & Xu, Y. (2019). Generating WUDAPT Level 0 data – Current status of production and evaluation. *Urban Climate*, 27(August 2018), 24–45. <https://doi.org/10.1016/j.uclim.2018.10.001>
- Bechtel, B., Alexander, P. J., Böhner, J., Ching, J., & Conrad, O. (2015). Mapping Local Climate Zones for a Worldwide Database of the Form and Function of Cities. *ISPRS International Journal of Geo-Information*, 4, 199–219. <https://doi.org/10.3390/ijgi4010199>
- Bueno, B., Norford, L., Hidalgo, J., & Pigeon, G. (2013). The urban weather generator. *Journal of Building Performance Simulation*, 6(4), 269–281. <https://doi.org/10.1080/19401493.2012.718797>
- Bueno, B., Roth, M., Norford, L., & Li, R. (2014). Computationally efficient prediction of canopy level urban air temperature at the neighbourhood scale. *Urban Climate*, 9, 35–53. <https://doi.org/10.1016/j.uclim.2014.05.005>
- C40 Cities. (2016). *Deadline 2020*. https://www.c40.org/wp-content/uploads/2021/07/Deadline_2020.pdf
- Ordenanza General de Urbanismo y Construcciones, Pub. L. No. D.S. N°47, OGUC (2022).
- Climate data. (2023). *Climate data*. <https://es.climate-data.org/america-del-sur/chile/ix-region-de-la-araucania/temuco-6152/>
- Corporación de Desarrollo Tecnológico. (2019). *Informe final de usos de energía de los Hogares Chile 2018*.
- Davenport G., A., Susan, C., Grimmond, B., & Oke, T. R. (2000). Estimating the roughness of cities and sheltered country. *American Meteorological Society*. <https://www.researchgate.net/publication/224001525>
- Grimmond, C. S. B. (1992). The suburban energy balance: Methodological considerations and results for a mid-latitude west coast city under winter and spring conditions. *International Journal of Climatology*, 12(5), 481–497. <https://doi.org/10.1002/joc.3370120506>
- Hong, T., Ferrando, M., Luo, X., & Causone, F. (2020). Modeling and analysis of heat emissions from buildings to ambient air. *Applied Energy*, 277(July), 115566. <https://doi.org/10.1016/j.apenergy.2020.115566>
- IEA. (2020). Energy Technology Perspectives 2020 - Special Report on Clean Energy Innovation. In *Energy Technology Perspectives 2020*. <https://doi.org/10.1787/ab43a9a5-en>
- INE. (2017). *Instituto Nacional de Estadística*. Proyecciones de Población. <https://regiones.ine.cl/araucania/estadisticas-regionales/sociales/demografia-y-vitales/proyecciones-de-poblacion>

- Khan, A., Chatterjee, S., & Wang, Y. (2021). Context and background of urban heat island. In *Urban Heat Island Modeling for Tropical Climates* (pp. 1–35). <https://doi.org/10.1016/B978-0-12-819669-4.00001-5>
- Li, H., Meier, F., Lee, X., Chakraborty, T., Liu, J., Schaap, M., & Sodoudi, S. (2018). Interaction between urban heat island and urban pollution island during summer in Berlin. *Science of the Total Environment*, 636, 818–828. <https://doi.org/10.1016/j.scitotenv.2018.04.254>
- Litardo, J., Palme, M., Borbor-Cordova, M., Caiza, R., Macias, J., Hidalgo-Leon, R., & Soriano, G. (2020). Urban Heat Island intensity and buildings' energy needs in Duran, Ecuador: Simulation studies and proposal of mitigation strategies. *Sustainable Cities and Society*, 62(July), 102387. <https://doi.org/10.1016/j.scs.2020.102387>
- López-Guerrero, R. E., Verichev, K., Moncada-Morales, G. A., & Carpio, M. (2022). How do urban heat islands affect the thermo-energy performance of buildings? *Journal of Cleaner Production*, 373. <https://doi.org/10.1016/j.jclepro.2022.133713>
- Mao, J., Yang, J. H., Afshari, A., & Norford, L. K. (2017). Global sensitivity analysis of an urban microclimate system under uncertainty: Design and case study. *Building and Environment*, 124, 153–170. <https://doi.org/10.1016/j.buildenv.2017.08.011>
- Martinez-soto, A., Vera-fonseca, M., & Valenzuela-toledo, P. (2021). Determination of The Intensity and Georeferencing of Urban Heat Islands in Temuco, Chile. *Research Square*, 1–22. <https://doi.org/10.21203/rs.3.rs-156219/v1>
- Matzarakis, A., Wetterdienst, D., Rutz, F., Matzarakis, A., & Rutz, F. (2006). RayMan: A TOOL FOR RESEARCH AND EDUCATION IN APPLIED CLIMATOLOGY. *8 Th CONFERENCE ON METEOROLOGY-CLIMATOLOGY-ATMOSPHERIC PHYSICS ATHENS*. <https://www.researchgate.net/publication/233759055>
- Meteochile. (2023). *Dirección Meteorológica de Chile*. <Http://Www.Meteochile.Gob.Cl/PortalDMC-Web/Index.Xhtml>. <http://www.meteochile.gob.cl/PortalDMC-web/index.xhtml>
- Municipalidad de Temuco. (2015). *ESTUDIO DE PAISAJE E IMAGEN URBANA*. <https://legacy.temuco.cl/wp-content/uploads/2018/12/Cap5-Imagen-Urbana.pdf>
- Nakano, A., Bueno, B., Norford, L., & Reinhart, C. F. (2015). Urban Weather Generator User Interface Development: New Workflow for Integrating Urban Heat Island Effect in Urban Design Process. *ICUC9 -9thInternational Conference on Urban Climate Jointly With12thSymposium on the Urban Environment*. <http://urbanmicroclimate.scripts.mit.edu>
- Oke, T. R. (2006). *INITIAL GUIDANCE TO OBTAIN REPRESENTATIVE METEOROLOGICAL OBSERVATIONS AT URBAN SITES*.
- Oke, T. R., Mills, G., Christen, A., & Voogt, J. A. (2017). *Urban climates* (C. U. Press, Ed.; First publ). Cambridge University Press.
- ONU. (2015). *Objetivos de Desarrollo – ONU*. <https://onu.org.gt/objetivos-de-desarrollo/>

- ONU. (2018). World Urbanization Prospects. In *Demographic Research* (Vol. 12).
<https://population.un.org/wup/publications/Files/WUP2018-Report.pdf>
- Palme, M., Inostroza, L., Villacreses, G., Lobato, A., & Carrasco, C. (2017). Urban weather data and building models for the inclusion of the urban heat island effect in building performance simulation. *Data in Brief*, 14(August), 671–675. <https://doi.org/10.1016/j.dib.2017.08.035>
- Peel, M. C., Finlayson, B. L., & McMahon, T. A. (2007). Updated world map of the Köppen-Geiger climate classification. *Hydrology and Earth System Sciences*, 1633–1644.
- Pérez-Fargallo, A., Bienvenido-Huertas, D., Rubio-Bellido, C., & Trebilcock, M. (2020). Energy poverty risk mapping methodology considering the user's thermal adaptability: The case of Chile. *Energy for Sustainable Development*, 58, 63–77.
<https://doi.org/10.1016/j.esd.2020.07.009>
- Quah, A. K. L., & Roth, M. (2012). Diurnal and weekly variation of anthropogenic heat emissions in a tropical city, Singapore. *Atmospheric Environment*, 46, 92–103.
<https://doi.org/10.1016/j.atmosenv.2011.10.015>
- Roy, J. P., Tschakert, H., Waisman, S., Abdul Halim, P. A.-A., Dasgupta, P., Hayward, B., Kanninen, M., Liverman, D., Okereke, C., Pinho, P. F., Riahi, K., & Rodriguez, A. G. S. (2018). *Sustainable Development, Poverty Eradication and Reducing Inequalities. In: Global Warming of 1.5°C. An IPCC Special Report on the impacts of global warming of 1.5°C above pre-industrial levels and related global greenhouse gas emission pathways, in the context of strengthening the global response to the threat of climate change, sustainable development, and efforts to eradicate poverty.*
<https://www.ipcc.ch/report/sr15/chapter-5-sustainable-development-poverty-eradication-and-reducing-inequalities/>
- Salvati, A., Monti, P., Coch Roura, H., & Cecere, C. (2019). Climatic performance of urban textures: Analysis tools for a Mediterranean urban context. *Energy and Buildings*, 185, 162–179. <https://doi.org/10.1016/j.enbuild.2018.12.024>
- Stewart, I. D., & Oke, T. R. (2012). Local climate zones for urban temperature studies. *Bulletin of the American Meteorological Society*, 93(12), 1879–1900. <https://doi.org/10.1175/BAMS-D-11-00019.1>
- Ulpiani, G. (2021). On the linkage between urban heat island and urban pollution island: Three-decade literature review towards a conceptual framework. *Science of the Total Environment*, 751, 141727. <https://doi.org/10.1016/j.scitotenv.2020.141727>
- UN-HABITAT. (2012). *STATE OF LATIN AMERICAN AND CARIBBEAN CITIES 2012 Towards a new urban transition.* <https://unhabitat.org/sites/default/files/download-manager-files/State%20of%20Latin%20American%20and%20Caribbean%20cities.pdf>
- UN-HABITAT. (2019). *UN-Habitat Strategic Plan 2020-2023.*
https://unhabitat.org/sites/default/files/documents/2019-09/strategic_plan_2020-2023.pdf

Verichev, K., & Carpio, M. (2020). Effects of climate change on variations in climatic zones and heating energy consumption of residential buildings in the southern Chile. *Energy & Buildings*, 215(109874). <https://doi.org/10.1016/j.enbuild.2020.109874>

Woong Kim, S., & Brown, R. D. (2021). Urban heat island (UHI) intensity and magnitude estimations: A systematic literature review. *Science of the Total Environment*, 779. <https://doi.org/10.1016/j.scitotenv.2021.146389>

Yang, X., Peng, L. L. H., Jiang, Z., Chen, Y., Yao, L., He, Y., & Xu, T. (2020). Impact of urban heat island on energy demand in buildings: Local climate zones in Nanjing. *Applied Energy*, 260(30), 114279. <https://doi.org/10.1016/j.apenergy.2019.114279>

Zhou, D., Zhao, S., Zhang, L., Sun, G., & Liu, Y. (2015). The footprint of urban heat island effect in China. *Scientific Reports*, 5, 2–12. <https://doi.org/10.1038/srep11160>

Communication aligned with the Sustainable Development Objectives

